SAINS TANAH – Journal of Soil Science and Agroclimatology

Journal homepage: http://jurnal.uns.ac.id/tanah

Characteristics of inceptisol ameliorated with rice husk biochar to glyphosate adsorption

Herviyanti[1]*, Amsar Maulana[2], Arestha Leo Lita[3] , Teguh Budi Prasetyo[1], Moli Monikasari[4], Ridho Ryswaldi[5]

[1] Department of Soil Science and Land Resources, Faculty of Agriculture, Universitas Andalas, Indonesia
[2] Ph.D. Students of Agricultural Science Postgraduate Universitas Andalas, Indonesia
[3] Magister Students of Soil Science Postgraduate Universitas Andalas, Indonesia
[4] Graduate of Soil Science, Agriculture Faculty, Universitas Andalas, Indonesia
[5] Department of Management, Faculty of Economics and Business, Universitas Andalas, Indonesia

ARTICLE INFO

Keywords:
Adsorption
Amelioration Technology
Inceptisol
Glyphosate
Rice Husk Biochar

Article history
Submitted: 2022-06-01
Accepted: 2022-11-25
Available online: 2022-12-31
Published regularly: Dec 2022

***** *Corresponding Author*
Email address:
herviyanti@agr.unand.ac.id

ABSTRACT

As an ameliorant, rice husk biochar (RHB) can improve soil quality and long-term carbon absorption and interaction with glyphosate during adsorption. This study investigated the ability of Inceptisol ameliorated with RHB to absorb glyphosate. Inceptisol ameliorated with 40^{-t} ha^{-1} RHB increased the soil surface charge (ΔpH) by improving soil pH H_2O, electrical conductivity, cation exchange capacity, and soil organic matter. Linear and nonlinear models showed that fitting Langmuir and Freundlich isotherms is suitable for this study. The isotherm adsorption of glyphosate sequentially occurs in the Freundlich and Langmuir models (Inceptisol + 40^{-t} ha^{-1} RHB > Inceptisol), where the Freundlich model (R^2 = 0.938) is dominated by glyphosate adsorption on Inceptisol + 40^{-t} ha^{-1} RHB with n of 0.46 and KF of 1.747 mg kg^{-1}, whereas the Langmuir model (R^2 = 0.8608) with Qm of 30.01 mg kg^{-1} and KL of 0.08 L mg^{-1} at a concentration level of 100 ppm and pH of the glyphosate solution 5.20 units. The glyphosate adsorption was also supported by changes in functional groups, where Fourier transform infrared spectroscopy shows a decrease in transmittance in the O-H; C=C; C-O; C-H, and mineral groups, indicating an increase in the adsorption capacity in Inceptisol ameliorated with 40^{-t} ha^{-1} RHB. This study indicated that the physicochemical properties of Inceptisol are important in controlling the glyphosate adsorption ability of RHB in soils.

How to Cite: Herviyanti, Maulana, A., Lita, A.L., Prasetyo, T.B., Monikasari, M., Ryswaldi, R. (2022). Characteristics of inceptisol ameliorated with rice husk biochar to glyphosate adsorption. Sains Tanah Journal of Soil Science and Agroclimatology, 19(2): 230-240. https://dx.doi.org/10.20961/stjssa.v19i2.61614

1. INTRODUCTION

Environmental contamination decreases soil quality by affecting the bio-physicochemical characteristics of the soil system. The existence of xenobiotic chemicals in soil bodies as pollutants is caused by various actions of farmers with excessive chemical concentrations that are not within their expected values. This is the primary cause of the expanding urbanization of pollutant compounds that should be held accountable for the pollution of water bodies and soils by xenobiotic compounds that are extensively distributed in the environment, including pesticides and other chemicals (Varjani et al., 2019). Pesticides have been and will continue to be used to manage plant-disturbing organisms such as insects, weeds, and diseases in various agricultural operations. Improper usage, as indicated by the manufacturer, has a more significant impact on non-target species via direct and indirect exposure. Approximately 2 million tons of pesticides are used globally, accounting for 65% of the pesticide market (De et al., 2014), with herbicides dominating the global market. Glyphosate (N-phosphonomethyl-glycine) is a common herbicide active ingredient used by farmers in horticulture (Figure 1). The annual global usage of glyphosate is estimated to be 600–750 thousand tons, with a projected increase to 740–920 thousand tons by 2025 (Caceres-Jensen et al., 2019; Maggi et al., 2020).

The World Health Organization has identified the teratogenicity of glyphosate chemicals in cultivated plants and people as a probable type of carcinogen development by

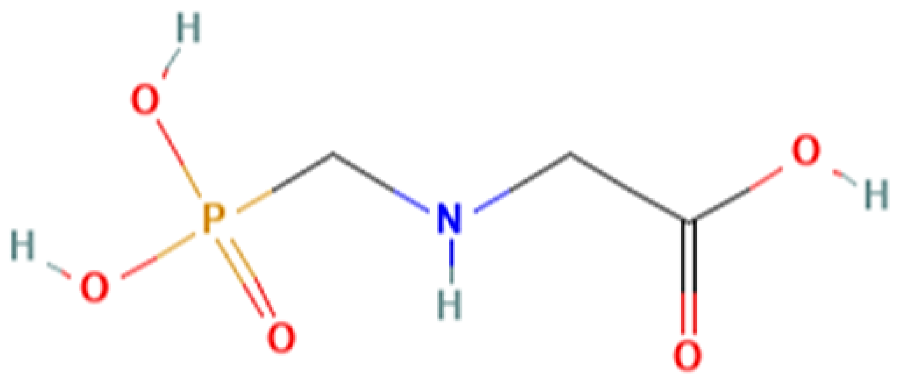

Figure 1. Structure and physicochemical properties of glyphosate (N-phosphonomethyl-glycine) (Tzanetou & Karasali, 2020)

application and metabolite ingestion (Flores et al., 2018; Tsamo et al., 2019). Glyphosate is highly harmful. It must be removed from the water–soil system as soon as possible. Chemical oxidation, electrolysis, biochemistry, adsorption, evaporation, and other standard procedures are currently used to remove glyphosate from soil. Soil is the most abundant growth medium on the planet and a natural adsorbent for pollutants, but its adsorption qualities and power must be improved. Soil's physical and chemical qualities as an adsorbent are highly dependent on its structure and content, which are characterized by a large surface area, abundant surface hydroxyl and silanol groups, high cationic exchange capacity, and chemical and mechanical stability (Okada et al., 2016; Viglašová et al., 2018; Wang et al., 2019). The majority of glyphosate sprayed enters the soil in its original form. Once in the soil, it may be absorbed by clay minerals and iron oxides (Orcelli et al., 2018; Pereira et al., 2019) or organic matter (Gros et al., 2019; Pereira et al., 2020).

Furthermore, glyphosate may be degraded by soil microorganisms (Zhan et al., 2018). Through the carboxyl and phosphonate groups, glyphosate interacts with peptides/proteins and soil organic matter. Furthermore, glyphosate may interact with metals in soils (Gros et al., 2019). Depending on the iron oxide makeup of the soil, glyphosate may be washed off more easily. However, because glyphosate binds to each surface plane of goethite with varying intensities, the interaction between glyphosate and iron oxides is highly complex (Ahmed et al., 2018). Research results vary and depend on the selected experimental conditions, such as the concentration of herbicides and the type of soil under study. However, note that adsorption technology that will be applied to soil to improve soil quality in the adsorption of glyphosate must be cost-effective, one of which is by using local wastes such as rice husks as raw materials for ameliorants such as biochar.

Biochar is prepared by the pyrolysis of waste or biomass in the absence or presence of oxygen, resulting in a carbon-rich charcoal composition (Shaaban et al., 2013). Biochar has many negative surface charges, surface functional groups, and other structural and textural qualities, including a large specific surface area, large pore volume, and high cationic exchange capacity. The physicochemical properties of biochar are mainly determined by the type of raw material, which is further modified by parameters such as techniques (Herviyanti et al., 2020; Maulana et al., 2022), particles (Lita et al., 2022), and temperature (Trigo et al., 2016) during the pyrolysis process. Biochar can be used as an ameliorant in amelioration technology for various purposes (Maulana et al., 2021), one of which is the rehabilitation of polluted soil such as glyphosate (Herath et al., 2019). Many researchers have recently explored the collaboration between biochar and soil to improve its properties and application domain in agriculture as well as against glyphosate adsorption (Premarathna et al., 2019; Wang et al., 2019; Yao et al., 2014). In the agricultural sector, this potential is developed sustainably. Soil and biochar are geo-biosorbents that can be used for soil restoration and provide an inexpensive procedure while reducing the environmental impact of agricultural and industrial wastes. This study investigated the glyphosate absorption ability of Inceptisol ameliorated with rice husk biochar (RHB).

2. MATERIALS AND METHODS

The research was conducted at the Laboratory of Chemistry and Soil Fertility, Faculty of Agriculture, Andalas University, Padang, from April to June 2021.

2.1 Soil Samples and Analyses

Soil samples were selected on the basis of maps of soil type and land use at the horticultural crop production center, namely, soil types with the order Inceptisol (Figure 2) from Sariak, Sungai Pua, Agam Regency in West Sumatra, Indonesia, with GPS coordinates of –0021'56'' LS and 100024'0'' BT. The soil samples were taken compositely at a depth of 0–20 cm with three replications and a sample weight of 1 kg for each repetition. Soil samples collected in the field were air-dried for 2 × 24 h before being crushed and sieved using a 2^{-mm} sieve. The soil sample was then weighed at 500^{-g} absolute dry equivalent, composited with 40^{-t} ha^{-1} RHB (Maulana et al., 2021) and incubated for two weeks. After the incubation, the soil analysis process is performed in the laboratory. Soil ana-

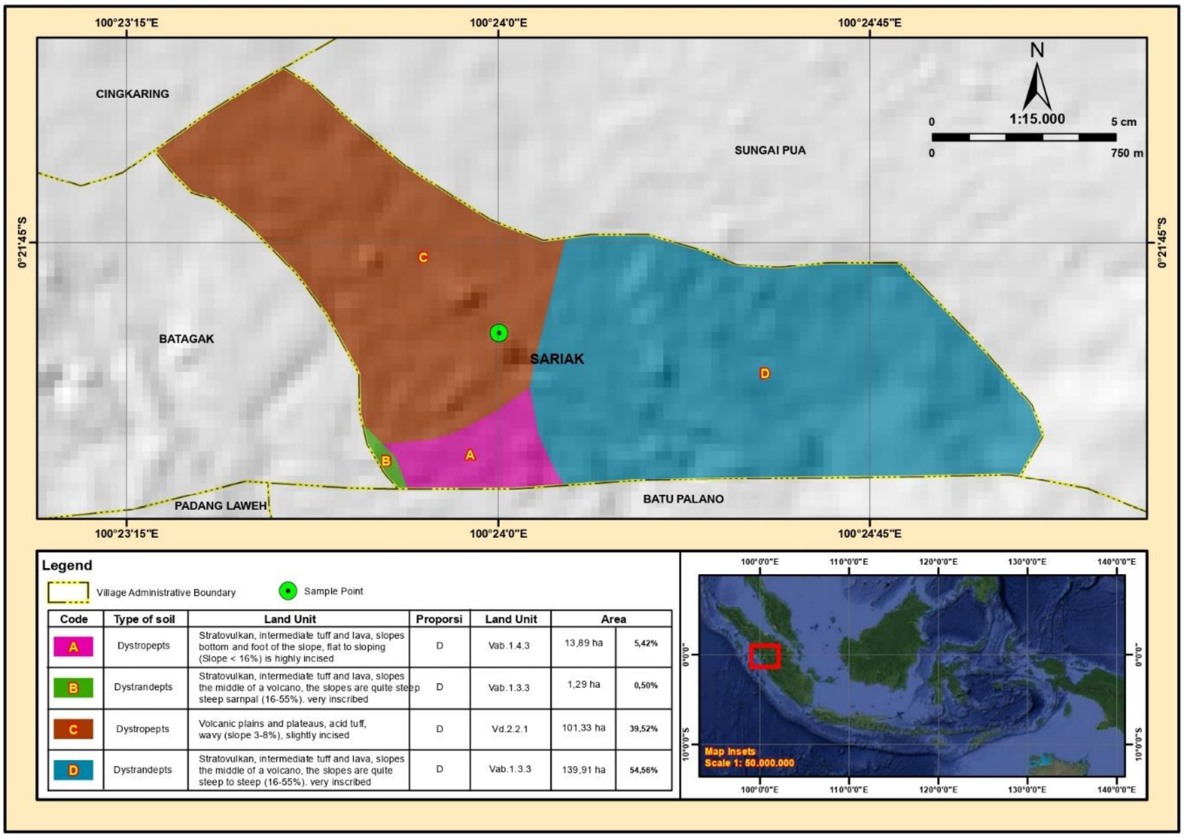

Figure 2. Map of soil types in Sariak, Sungai Pua Agam Regency, West Sumatra Indonesia

lysis refers to the goal of studying the surface charge activity of geo-biosorption (Inceptisol - RHB) and geosorption (Inceptisol) using the following parameters: clay content, pH H_2O (pH-active), pH KCl (pH-potential), electrical conductivity (EC), cation exchange capacity (Maggi et al.), mineral, soil organic matter (SOM). Fourier transform infrared (FTIR) reflectance spectra were collected between 500 and 4000 cm^{-1} (Singh et al., 2017).

2.2 RHB Productions

Rice husk is a waste from the rice milling industry. RHB is produced using the Drum method through a pyrolysis process. Pyrolysis was performed in iron drums with a diameter of 58 cm, a height of 86 cm, and a capacity of 200 liters and combined with the Kon-Tiki method (Herviyanti et al., 2022) at temperatures up to 650 ^{0}C. The maximum pyrolysis temperature was kept constant for 45 min to ensure the completion of the final process.

2.3 Glyphosate Solution

The glyphosate solution was prepared with five concentration levels (0, 1, 5, 10, 50, and 100 mg L^{-1}). It was prepared by dissolving the herbicide (Roundup Biosorb 486 SL) in 0.01-M $CaCl_2$. The 100^{-mg} L^{-1} glyphosate concentration was obtained by adding 0.14 mL of herbicide (Roundup Biosorb 486 SL) to 500 mL of 0.01^{-M} $CaCl_2$. Meanwhile, concentrations of 1-, 5-, 10-, and 50^{-mg} L^{-1} glyphosate was made from the volume of each concentration of 3.5, 17.5, 35, and 175 mL in 500 mL of 0.01^{-M} $CaCl_2$ (Glass, 1981).

2.4 Batch Adsorption Experiments

The adsorption experiment was conducted by mixing 0.5 g of adsorbent with 20 mL of the glyphosate solution in a closed 25^{-mL} glass cylindrical tube in an isothermal test. At the concentrations of 1, 5, 10, 50, and 100 mg L^{-1}, the mixture was stirred on a rotary shaker at 250 rpm for 24 h at laboratory temperature (25 ^{0}C). The samples were centrifuged at 4000 rpm for 30 min. The model was filtered using Whatman No. 1 filter paper. The pH of the filtrate solution was measured at each concentration, and the equilibrium concentration of glyphosate remaining in the solution was determined using a UV–Vis spectrophotometer at a wavelength of 830 nm with complexing (Glass, 1981).

The amount of glyphosate adsorbed by different adsorbents was calculated by Eq. (1) to calculate the adsorption capacity (Q_e) and effectivity (% R) from Eq. (2).

$$Q_e = \frac{(C_O - C_e)}{m} * V, \quad [1]$$

$$\% R = = \frac{(C_O - C_e)}{C_O} * 100\%, \quad [2]$$

where Qe (mg kg^{-1}) represents the adsorption capacity, Co and Ce (mg L^{-1}) denote the initial and final glyphosate concentrations, respectively, m (g) represents the mass of Inceptisol and Inceptisol + 40^{-t} ha^{-1} RHB, and V (L) represents the volume of the glyphosate solution. Two isothermal models Langmuir and Freundlich were used to adjust the experimental data. Correspondingly, the following linearized and nonlinearized forms of these models are applied for the adsorption isotherm Freundlich (Eq. 3) and Langmuir models (Eq. 4):

Linear: $\text{Log } Q_e = \text{Log } K_F + n(\text{Log } C_e)$; Nonlinear: $Q_e = K_F C_e^n$ [3]

Linear: $\frac{Ce}{Q_e} = \frac{1}{Q_m} Ce + \frac{1}{Q_m Kl}$; Nonlinear: $Q_e = Q_m K_L C_e / 1 + K_L C_e$; [4]

where C_e (mg L^{-1}) denotes the equilibrium concentration of the glyphosate solution, Q_e and Q_m (mg kg^{-1}) denote the amounts adsorbed and maximum adsorption capacity, respectively, and KL represents the Langmuir constant (L mg^{-1}); KF denotes the Freundlich affinity coefficient (mg kg^{-1}) or adsorption capacity of the adsorbent, and n indicates the favorableness (n > 1) of the adsorption process.

3. RESULTS

3.1 Characteristics of Infrared Spectroscopy

The FTIR spectrum obtained from Inceptisol and Inceptisol + 40^{t} ha^{-1} RHB is shown in Figure 3 and Table 1. Figure 3A.1 shows that the FTIR spectrum of Inceptisol with a band at 1022.11 cm^{-1}/66.40% could be attributed to 3282.05 cm^{-1}/88.44%, which could be assigned to the internal and internal hydroxyl group strain vibrations. The band at 1629.91 cm^{-1}/88.95% is associated with deformation vibrations of water absorbed at the clay interlayer and is associated with strain vibrations of C-O and C-C, corresponding to the carbonyl and aromatic rings, respectively. The FTIR band at 546.79 cm^{-1}/50.50% was associated with stretching Si-O-Al bonds (Mineral, e.g., kaolinite and smectite). The functional group that appeared was the alcoholic C-O strain and aromatic C-H bending vibrations.

The FTIR spectrum of Inceptisol + 40^{t} ha^{-1} RHB showed the same vibrations as Inceptisol, which were 3280.62 cm^{-1}/87.48%, 1630.83 cm^{-1}/87.98%, 1025.50 cm^{-1}/63.19%, and 546.97 cm^{-1}/48.26% bands. The Inceptisol + 40^{t} ha^{-1} RHB exhibited a decrease in transmittance in each band, indicating an increase in adsorption capacity through the administration of 40^{t} ha^{-1} RHB-ameliorated Inceptisol. The FTIR spectrum of Inceptisol + 40^{t} ha^{-1} RHB also revealed a band at 3280.62 cm^{-1}/87.48%, which could be assigned to the internal and internal hydroxyl group strain vibrations. The band at 1630.83 cm^{-1}/87.98% is associated with the water deformation vibrations absorbed in the clay interlayer. It is associated with the C-O and C-C strain vibrations corresponding to the carbonyl and aromatic rings. On the other hand, an absorption band of 1025.50 cm^{-1}/63.19% also appears, which is associated with C-O (alcohols, ethers, carboxylic acid, esters) and aromatic C-H bending vibrations. The FTIR band at 546.97 cm^{-1}/48.26% was associated with the mineral band strain (e.g., kaolinite) (Figure 3B.1 and Table 3).

Table 1 and Figure 3A.2 and B.2 show that the pesticide adsorption process affected changes in the adsorption bands of the adsorbents in glyphosate adsorption. In the FTIR spectrum of Inceptisol, there was only a decrease in transmittance, which indicated that the intensity of each group that appeared was 3272.74 cm^{-1}/87.96% (O-H: Hydrogen-bonded alcohols, phenols), 1627.08 cm^{-1}/88.47% (In C=C: Alkenes), 1005.72 cm^{-1}/65.20% (C-O: Alcohols, ethers, carboxylic acid, esters), and 548.60 cm^{-1}/48.80% (Minerals), after the adsorption of glyphosate and the loss of mineral groups after the adsorption process on Inceptisol + 40^{t} ha^{-1} RHB. However, there was high-intensity power in the O-H, C=C, and C-O groups with a decrease in transmittance to 3282.33 cm^{-1}/86.91%, 1627.25 cm^{-1}/87.73%, and 1017.08 cm^{-1}/62.29% after the adsorption process on Inceptisol + 40^{t} ha^{-1} RHB.

3.2 Physicochemical Characteristics of Inceptisol and Ameliorated Inceptisol with Rice Husk Biochar

RHB is used for amelioration technology and as an adsorbent in glyphosate adsorption. The clay content of Inceptisol is 5.90%, which is the main component of the soil surface charge (Table 2). Table 2 shows the pH of H_2O and KCl Inceptisol at 4.97 and 4.73, respectively, whereas an increase of 0.70 and 0.34 occurred with the application of 40^{t} ha^{-1} RHB on Inceptisol. The ΔpH value describes the surface charge activity in the soil, which aims to support the adsorption process in the soil. ΔpH increased by 0.36 with the application of 40^{t} ha^{-1} RHB on Inceptisol (Table 2). This indicates that the increase in surface charge activity and the positive value of Ph suggest that negative charges dominate the soil. The EC value of the soil increased by 0.03 dS m^{-1}, whereas the EC of Inceptisol was 0.08 dS m^{-1} and increased by 0.11 dS m^{-1}. The amelioration of 40^{t} ha^{-1} RHB on Inceptisol can increase CEC 2 times from Inceptisol, which was 46.06 cmol kg^{-1} from 30.25 to 76.27 cmol kg^{-1} (Table 2). Table 2 shows that the mineral composition and SOM will change with the application of organic or inorganic materials to the ameliorated soil, where 40^{t} ha^{-1} RHB on Inceptisol reduces ash content and increases SOM, respectively -/+ 7.4%.

Table 1. Spectral band assignments of Inceptisol and Inceptisol ameliorated with rice husk biochar, before and after adsorption.

Before Adsorption		After Adsorption		Description of Bond (Type of Compound – Intensity)*
Inceptisol	Inceptisol + 40 t ha^{-1} RHB	Inceptisol	Inceptisol + 40 t ha^{-1} RHB	
	Wavenumbers / Transmittance (cm^{-1}/ %)			
3282.05/ 88.44	3280.62/ 87.48	3272.74/ 87.96	3282.33/ 86.91	O-H (Hydrogen-bonded alcohols, phenols) – Variabel, sometimes broad
1629.91/ 88.95	1630.83/ 87.98	1627.08/ 88.47	1627.25/ 87.73	C=C (Alkenes) – Variabel
1022.11/ 66.40	1025.50/ 63.19	1005.72/ 65.20	1017.08/ 62.29	C-O (Alcohols, ethers, carboxylic acid, esters) – Strong
546.79/ 50.50	546.97/ 48.26	548.60/ 48.80	-	Mineral (e.g., kaolinite, CaO, MgO, and others)

Table 2. Soil surface charge activity of Inceptisol and Inceptisol ameliorated with rice husk biochar (RHB)

Soil	Clay	pH H_2O	pH KCl	ΔpH[a]	EC	CEC	Mineral	SOM
	%	unit			dS m^{-1}	$cmol_{(+)}$ kg^{-1}	%	
Inceptiols		4.97	4.73	0.24	0.08	30.25	70.80	29.20
Inceptisol + 40 t ha^{-1} RHB	5.90	5.67	5.07	0.60	0.11	76.27	63.40	36.60

Remarks: EC = Electrical conductivity; CEC = Cation exchange capacity; SOM = Soil organic matter.
a : ΔpH = pH H_2O – pH KCl

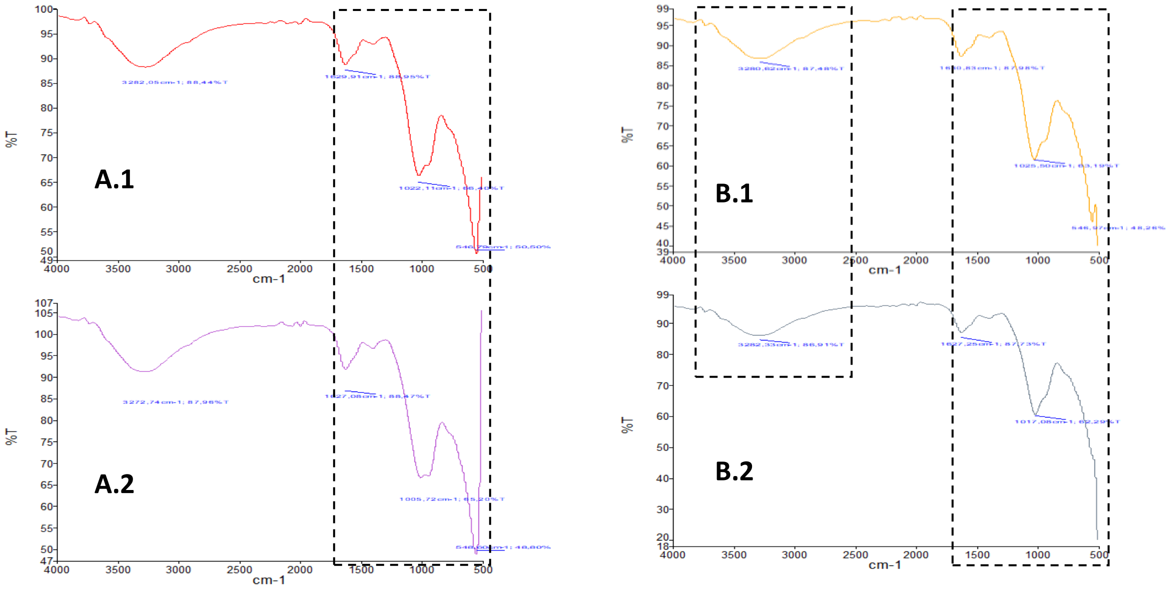

Figure 3. FTIR spectra of Inceptisol (A) and Inceptisol ameliorated with rice husk biochar (B), before (1) and after (2) adsorption

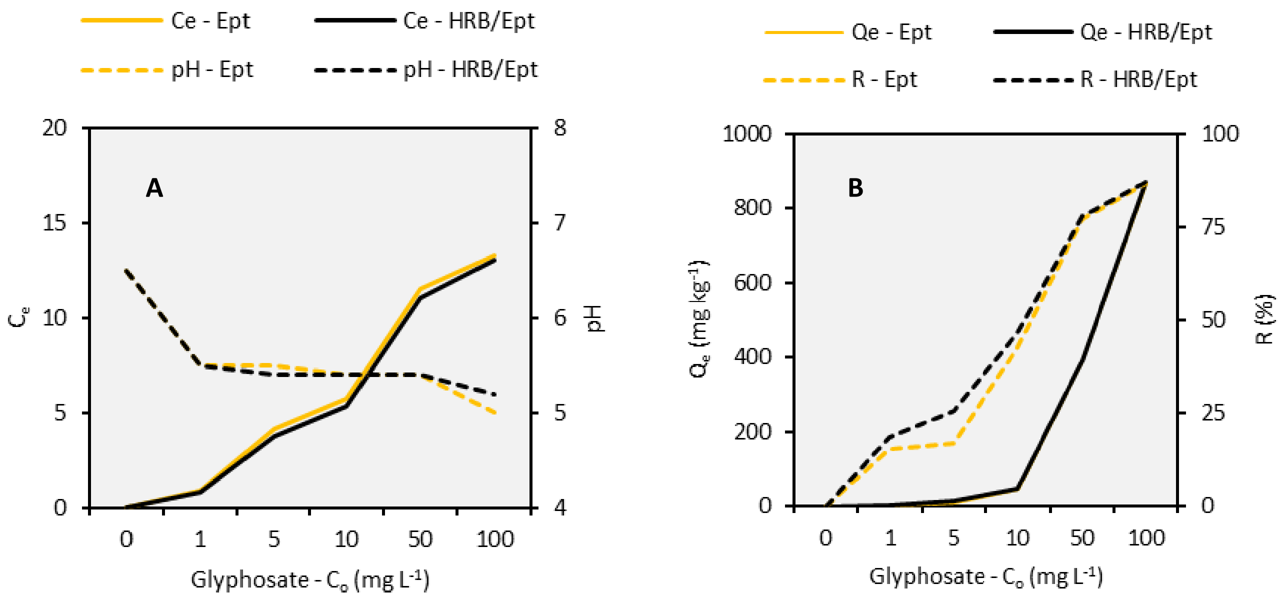

Figure 4. (A) Equilibrium concentration glyphosate (Ce) and pH during the adsorption process on RHB; Inceptisol and Inceptisol ameliorated with rice husk biochar and (B) Glyphosate adsorption capacity (Qe) and removal effectivity (R) of Inceptisol and RHB/Inceptisol, where: C0 = 1–100 mg L^{-1}; Absorbent mass = 0.5 g; adsorption temperature = 25^{0}C; Glyphosate volume = 5 mL; particle size = 500µm and agitation speed/time = 250 rpm/24 hour.

3.3 Glyphosate Adsorption Behavior

The equilibrium concentration of glyphosate increases as the glyphosate concentration increases. Nevertheless, it decreases the pH of the solution during the adsorption process (Figure 4), where the highest concentration of glyphosate for Inceptisol and Inceptisol + 40^{t} ha^{-1} RHB had the same capacity at 100 ppm. Figure 4A shows that the pH of the solution during the adsorption process is critical to analyze because it affects the adsorption of glyphosate in the CaCl2 solution. The decrease in pH was influenced by an increase in the glyphosate concentration with stability at concentrations of 1–50 ppm in Inceptisol and Inceptisol + 40^{t} ha^{-1} RHB (Figure 4A).

Figure 4B shows that the adsorption of glyphosate on Inceptisol and Inceptisol + 40^{t} ha^{-1} RHB shows that the adsorption capacity of glyphosate increased gradually at low glyphosate concentrations (1^{-10} mg L^{-1}), then increased sharply (10–100 mg L^{-1}), and reached the peak point of adsorption capacity at a concentration level of 100 mg L^{-1} of glyphosate each 869.29 mg kg^{-1}. This is also seen in the adsorption effectiveness that occurs in the two types of adsorbents, where the energy of each adsorption is 86.68% (Inceptisol) and 86.93% (Inceptisol + 40^{t} ha^{-1} RHB). Inceptisol + 40^{t} ha^{-1} RHB exhibited the best performance in terms of glyphosate adsorption capacity and effectiveness compared with Inceptisol without amelioration (Figure 4B).

3.4 Isotherms Adsorption

The isotherm model suitable for the adsorption process was selected in the model with an R^2 value. The isotherm's linear and nonlinear model parameters are shown in Figure 5 and Table 3. The e R^2 of the linear and nonlinear model isotherms Freundlich and Langmuir (Table 3) is suitable for Inceptisol and Inceptisol + 40^{t} ha^{-1} RHB. The R^2 values for each model can be ordered as follows: Freundlich > Langmuir on Inceptisol + 40^{t} ha^{-1} RHB > Inceptisol for each equation with a value of R^2 = 0.938 > R^2 = 0.9011 (Figure 5A) and R^2 = 0.995 > R^2 = 0.997 (Figure 5B).

Figure 5A shows that the Langmuir linear model (R^2 = 0.8608) was dominated by the glyphosate adsorption process on soil amelioration with Inceptisol + 40^{t} ha^{-1} RHB with Q_m of 30.01 mg kg^{-1} and K_L of 0.082 L mg^{-1} (Figure 5B), at adsorption efficiency of 86.93%. In comparison, the Freundlich model (R^2 = 0.938) was dominated by the glyphosate adsorption process on Inceptisol + 40^{t} ha^{-1} RHB with a value of n (0.46) and K_F (1.75 L mg^{-1}) at an adsorption efficiency of 86.94%, at a concentration level of 100 ppm and pH of the solution during the adsorption process of 5.20 (Figure 4A).

4. DISCUSSION

The characteristics of the soil surface charge activity of Inceptisol and Inceptisol ameliorated with 40^{t} ha^{-1} RHB are shown in Table 2, where clay is the main component of the soil surface charge on clay minerals (Preocanin et al., 2016) The increase in soil pH and CEC due to 40^{t} h^{-1} RHB amelioration was due to the influence of OH ions donated by RHB to the soils. According to Mindari et al. (2014), the complexation of H^+ and OH^- on the surface of soil particles can affect the absorption of other cations and anions. On the other hand, there was also an increase in EC, where according to Adil et al. (2012), an increase in EC in soil by RHB carries a negative charge, so it can move in an electric field externally with an increase in single charged ions that causing an electric field. Changes in the electrochemical properties of clays are closely related to the amount of aluminum hydroxy complexes incorporated in the clays and their chemical composition and charge properties. Many hydroxy-Al species exist in partially neutralized Al ion solutions used to coat clays, and their loads can vary. The number of interlayers on the CEC affects the zero charge point on each adsorbent used in the adsorption process.

Table 3. Linear and nonlinear plot of Isotherms adsorption with Freundlich and Langmuir model in Inceptisol and Inceptisol ameliorated with rice husk biochar (RHB)

Models	Soil	Linear Parameters [Log Q_e = Log K_F + n(Log C_e)]		Nonlinear Parameters [$Q_e = K_F C_e^{1/n}$]			
		n	K_F (mg Kg^{-1})	Equational:	n	K_F	
Freundlich	Inceptisol	0.44	1.194	y = 2.2588x + 0.0769 R^2 = 0.9011	5,116	0,001504	
	Inceptisol + 40 t ha^{-1} RHB	0.46	1.747	y = 2.1847x + 0.2422 R^2 = 0.938	4,731	0,004534	
Models	Soil	Linear Parameters [C_e/Q_e = (1/Q_m.Ce+ 1/Q_m.K_L]		Nonlinear Parameters		[Q_e = Q_m.K_L .C_e/ (1+K_L.Ce]	
		Q_m (mg/kg)	K_L (L mg^{-1})	Equational:	Q_m	K_L	R^2
Langmuir	Inceptiols	21.17	0.079	y= -0.0451x +0.5644 R^2 = 0.8298	192812	0.00023	0.9800
	Inceptisol + 40 t ha^{-1} RHB	30.01	0.082	y = -0.0331x + 0.4026 R^2 = 0.8608	222611	0.00021	0.9778

Remarks: Freundlich : [n = 1/b; K_F = 10^a] and Langmuir : [Q_m = 1/b; K_L = b/a]

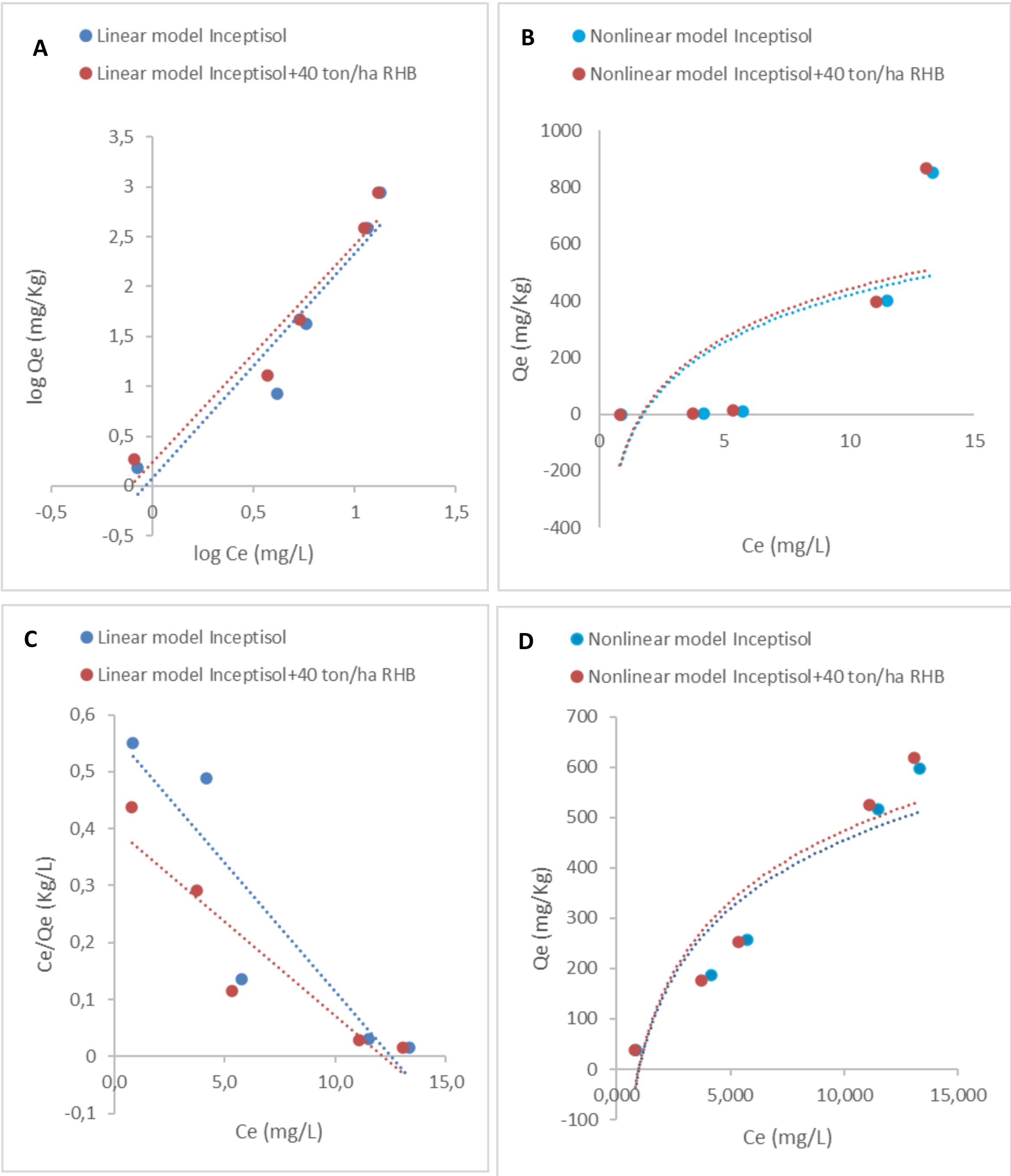

Figure 5. Linear plot of Freundlich linear model (A) Freundlich nonlinear model (B) Langmuir linear model (C) Langmuir nonlinear model (D) isotherm on the adsorption of glyphosate with Inceptisol and Inceptisol ameliorated with rice husk biochar (RHB).

The surface charge activity becomes essential in the adsorption process to determine the type of charge on the ameliorant surface at a certain ΔpH and its interaction with glyphosate. Analysis of the ΔpH value is also essential to describe the surface charge and positive and negative values on the results of reducing the pH H_2O, along with pH KCl, of the soil. If the ΔpH value is positive, the negative charge is dominant on the colloidal surface of the soil, and vice versa. The positive control dominates if the value is negative (Table 2). According to Mujinya et al. (2010), positive or negative ΔpH values indicate the presence of positive or negative net charges in colloids, respectively. The pH value of the solution during glyphosate adsorption is also significant to analyze because it also describes the shape of the charge on glyphosate (Figure 6A). This is because glyphosate is a polar molecule affected by the pH value. According to Sidoli et al. (2016) and Tzanetou and Karasali (2020), glyphosate is a small amphoteric molecule with three polar functional groups. These are the linearly organized phosphonomethyl, amine, and carboxymethyl groups. Glyphosate is an ionic compound (log KOW = 3.20), highly polar, and soluble in water (10.5 g L^{-1} at 20°C) due to the presence of those groups in its structure. Glyphosate is a polyprotic acid with four pKa values, namely, 0.7, 2.2, 5.9, and 10.6, 8, indicating that the molecule's

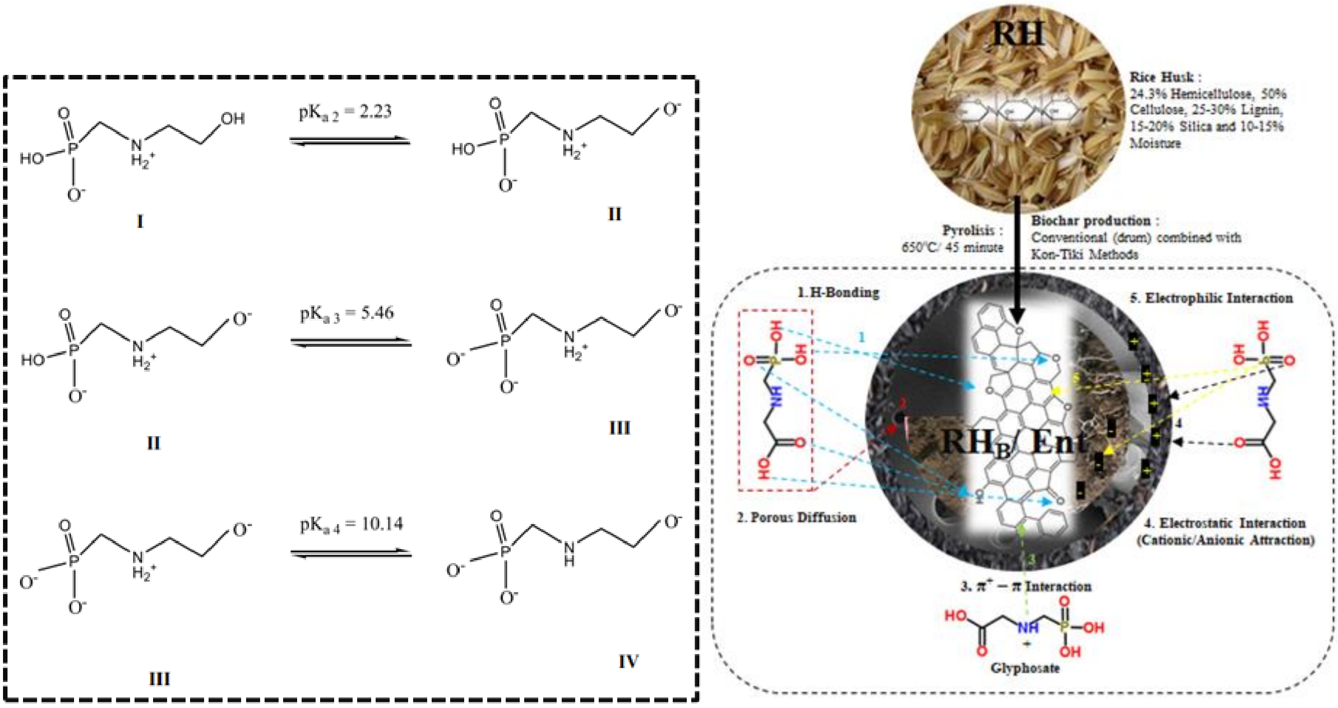

(A) **(B)**

Figure 6. (A) Ionic state of glyphosate as a function of pH (Tévez & Afonso, 2015) and (B) Prediction of glyphosate adsorption mechanism on Inceptisol ameliorated with rice husk biochar (RHB).

speciation is affected by the pH of the solution. AMPA has three pKa values: 0.9, 5.6, and 10.2. Monovalent and divalent anions are the most abundant species in soils.

The adsorption process can occur by forming a surface complex through the three phosphonate groups and coordinating OH, O, NH, and P with the adsorbent surface (Tévez & Afonso, 2015). These are influenced by the density of the active site of the adsorbent used and the specific surface area that can affect the adsorption capacity of glyphosate. This increase in adsorption may be due to an increase in the surface area and thus the number of active sites (Premarathna et al., 2019). In the soil, biochar undergoes various oxidation reactions that increase oxygen-containing functional groups such as phenol and carboxyl on the biochar surface. Therefore, biochar can have more glyphosate adsorption sites than fresh biochar. This explains how the incubation process of biochar in the soil affects the adsorption capacity, variations in soil chemical properties such as pH, CEC, and SOM (Table 2), and changes in functional groups before and after adsorption (Tables 1 and Figure 2). According to Herviyanti et al. (2022), biochar can increase pH, CEC, and SOM due to an increase in the negative charge contributed by the phenol and carboxyl groups and high carbon content in biochar (22%–52%). This plays a vital role in increasing the glyphosate adsorption capacity of Inceptisol + 40^{-t} ha^{-1} RHB. According to Kumari et al. (2016), the high prevalence of soil + biochar interactions, which include absorption sites in clay and amorphous oxides at higher levels of biochar application, play an essential role in biochar + soil interactions during glyphosate adsorption.

The isotherm adsorption was studied to determine the type of glyphosate layer formed on the soil's surface and the adsorption mechanism and to provide information about the maximum adsorption capacity (Gupta et al., 2019). This study used two adsorption isotherm models: Freundlich and Langmuir models. The suitable isotherm model for the adsorption process was selected on the basis of a model with an R^2 value close to 1 (Derakhshan et al., 2013). A high coefficient of determination (R^2) means a better prediction ability for the proposed research model (López-Luna et al., 2019). Thus, R^2 of the nonlinear model for the Freundlich and Langmuir isotherm adsorptions is fitting or suitable for explaining glyphosate adsorption, allowing for a more accurate prediction of the adsorption process or mechanism. The adsorption processes can co-occur (simultaneously) or sequentially. In the glyphosate adsorption on Inceptisol and Inceptisol + 40^{-t} ha^{-1} RHB, the adsorption mechanism begins with the adsorbate around the adsorbent surface reacting by "sticking" to the adsorbent surface (or this process can be referred to as physical adsorption by following the Freundlich isotherm mechanism). Glyphosate can adhere to the pores in the soil and biochar. Inceptisol with 40^{-t} ha^{-1} RHB input showed a higher R^2 value (Table 3) than those without biochar input. The material's structure, composed of cellulose and lignin, will naturally have a porous structure, enabling the material to be used as an adsorption medium (Aisyahlika et al., 2018). Rice husk has 35% cellulose and 20% lignin (Ma'ruf et al., 2017) thus, the presence of RHB in the soil can increase the space for absorption adsorbed.

Furthermore, the adsorption process runs slowly, and there is a balance between glyphosate and the adsorbent surface. Chemical reactions dominate the sorption process through different functional groups of the adsorbate and adsorbent, thereby describing the Langmuir isotherm mechanism. The mechanism of the herbicide adsorption reaction in the soil is primarily determined by the functional groups, both in soil minerals and in organic soil components. The clay content and organic elements in Inceptisol generally have active groups on the surface, such as–OH, according to the FTIR results presented in Fig. 3A. This group has a negative charge and binds to the amine group of glyphosate, which is positively charged, resulting in a chemical bond and the adsorption process. However, the clay content in Inceptisol is relatively low (5.90%), so it needs support or other negatively charged groups, such as those found in organic materials such as biochar. RHB has alumina silicate (Si-O-Si) (Hossain et al., 2017), which increases its adsorption ability. This is consistent with Sudirja et al. (2015) that functional groups that play an active role in herbicide adsorption include silanol groups (Si-OH), siloxanes (Si-O-Si), alumina silicate (Si-O-Al), and carboxylate groups (-COOH). The increase in adsorption ability when using adding RHB to Inceptisol is indicated by the R^2 value, which is greater than that when using only Inceptisol. This is also supported by the higher value of Qe (adsorption capacity). Thus, the adsorption mechanism occurs sequentially through the Freundlich and Langmuir isotherms.

The Langmuir model describes the soil and glyphosate that form a single layer in the adsorption process. All sites are the same, the soil surface is homogeneous, and the heat of adsorption is independent of the closure of the surface active sites (Kassimi et al., 2021). In contrast, the Freundlich model shows that the soil surface is heterogeneous due to a multilayer between the glyphosate molecules and the soil surface. The adsorption of glyphosate to Inceptisol and Inceptisol + 40^{-t} ha^{-1} RHB is shown in the linearized Freundlich and Langmuir model described in Figure 5, and the isotherm constants and correlation coefficients extracted from the plots are listed in Table 3. Previous studies have indicated that the mechanism of glyphosate adsorption on Inceptisol and Inceptisol + 40^{-t} ha^{-1} RHB are relatively different. Based on the R^2 values, the Freundlich and Langmuir models seem suitable to describe glyphosate adsorption by Inceptisol and ameliorated Inceptisol with 40^{-t} ha^{-1} RHB. This shows that the process of glyphosate adsorption by Inceptisol and Inceptisol ameliorated with 40-t ha^{-1} RHB is considered good for glyphosate adsorption.

5. CONCLUSION

Inceptisol ameliorated with 40^{-t} ha^{-1} RHB increased the soil surface charge (ΔpH) by improving soil pH H_2O, electrical conductivity, cation exchange capacity, and soil organic matter. Linear and nonlinear models showed that fitting Langmuir and Freundlich isotherms is suitable for this study. The isotherm adsorption of glyphosate sequentially occurs in the Freundlich and Langmuir models (Inceptisol + 40^{-t} ha^{-1} RHB > Inceptisol), where the Freundlich model (R^2 = 0.938) is dominated by glyphosate adsorption on Inceptisol + 40^{-t} ha^{-1} RHB with n of 0.46 and K_F of 1.747 mg kg^{-1}, whereas the Langmuir model (R^2 = 0.8608) with Q_m of 30.01 mg kg^{-1} and K_L of 0.08 L mg^{-1} at a concentration level of 100 ppm and pH of the glyphosate solution 5.20 units. The glyphosate adsorption was also supported by changes in functional groups, where Fourier transform infrared spectroscopy shows a decrease in transmittance in the O-H; C=C; C-O; C-H, and mineral groups, indicating an increase in the adsorption capacity in Inceptisol ameliorated with 40^{-t} ha^{-1} RHB. This study indicated that the physicochemical properties of Inceptisol are important in controlling the glyphosate adsorption ability of RHB in soils.

Acknowledgments

We were thankful for the financing of this research, which was provided by PNBP Andalas University (PDU-KRPGB) under Research Contract No: T/4/UN.16.17/PP.Pangan-KRP1GB/LPPM/2021 – 30th March 2021.

Declaration of Competing Interest

The authors declare that no competing financial or personal interests that may appear and influence the work reported in this paper.

References

Adil, A., Canan, K., & Metin, T. (2012). Humic acid application alleviate salinity stress of bean (Phaseolus vulgaris L.) plants decreasing membrane leakage. *African Journal of Agricultural Research*, *7*(7), 1073-1086. https://academicjournals.org/article/article1400835695_Aydin%20et%20al.pdf.

Ahmed, A. A., Leinweber, P., & Kühn, O. (2018). Unravelling the nature of glyphosate binding to goethite surfaces by ab initio molecular dynamics simulations. *Physical Chemistry Chemical Physics*, *20*(3), 1531-1539. https://pubs.rsc.org/en/content/articlelanding/2018/cp/c7cp06245a.

Aisyahlika, S. Z., Firdaus, M. L., & Elvia, R. (2018). Kapasitas adsorpsi arang aktif cangkang Bintaro (Cerbera odollam) terhadap zat warna sintetis Reactive RED-120 dan Reactive BLUE-198. *Alotrop*, *2*(2), 148-155. https://ejournal.unib.ac.id/index.php/alotropjurnal/article/view/7483.

Caceres-Jensen, L., Rodríguez-Becerra, J., Sierra-Rosales, P., Escudey, M., Valdebenito, J., Neira-Albornoz, A., . . . Villagra, C. A. (2019). Electrochemical method to study the environmental behavior of Glyphosate on volcanic soils: Proposal of adsorption-desorption and transport mechanisms. *Journal of hazardous materials*, *379*, 120746. https://doi.org/10.1016/j.jhazmat.2019.120746.

De, A., Bose, R., Kumar, A., & Mozumdar, S. (2014). *Targeted delivery of pesticides using biodegradable polymeric nanoparticles*. Springer. https://doi.org/10.1007/978-81-322-1689-6

Derakhshan, Z., Baghapour, M. A., Ranjbar, M., & Faramarzian, M. (2013). Adsorption of methylene blue dye from aqueous solutions by modified pumice stone: kinetics and equilibrium studies. https://doi.org/10.17795/jhealthscope-12492.

Flores, F. M., Torres Sánchez, R. M., & dos Santos Afonso, M. (2018). Some aspects of the adsorption of glyphosate and its degradation products on montmorillonite. *Environmental Science and Pollution Research*, *25*(18), 18138–18146. https://doi.org/10.1007/s11356-018-2073-4.

Glass, R. L. (1981). Colorimetric determination of glyphosate in water after oxidation to orthophosphate. *Analytical Chemistry*, *53*(6), 921-923. https://doi.org/10.1021/ac00229a048.

Gros, P., Ahmed, A. A., Kühn, O., & Leinweber, P. (2019). Influence of metal ions on glyphosate detection by FMOC-Cl. *Environmental monitoring and assessment*, *191*(4), 1-12. https://doi.org/10.1007/s10661-019-7387-2.

Gupta, N. K., Gupta, A., Ramteke, P., Sahoo, H., & Sengupta, A. (2019). Biosorption-a green method for the preconcentration of rare earth elements (REEs) from waste solutions: A review. *Journal of Molecular Liquids*, *274*, 148-164. https://doi.org/10.1016/j.molliq.2018.10.134.

Herath, G. A. D., Poh, L. S., & Ng, W. J. (2019). Statistical optimization of glyphosate adsorption by biochar and activated carbon with response surface methodology. *Chemosphere*, *227*, 533-540. https://doi.org/10.1016/j.chemosphere.2019.04.078.

Herviyanti, Maulana, A., Lita, A., Prasetyo, T., & Ryswaldi, R. (2022). Characteristics of biochar methods from bamboo as améliorant. IOP Conference Series: Earth and Environmental Science, https://doi.org/10.1088/1755-1315/959/1/012036

Herviyanti, H., Maulana, A., Prima, S., Aprisal, A., Crisna, S., & Lita, A. (2020). Effect of biochar from young coconut waste to improve chemical properties of ultisols and growth coffee [Coffea arabica L.] plant seeds. IOP Conference Series: Earth and Environmental Science, https://doi.org/10.1088/1755-1315/497/1/012038

Hossain, S. S., Mathur, L., Singh, P., & Majhi, M. R. (2017). Preparation of forsterite refractory using highly abundant amorphous rice husk silica for thermal insulation. *Journal of Asian Ceramic Societies*, *5*(2), 82-87. https://doi.org/10.1016/j.jascer.2017.01.001.

Kassimi, A., Achour, Y., Himri, M., Laamari, M. R., & Haddad, M. (2021). High efficiency of natural Safiot Clay to remove industrial dyes from aqueous media: Kinetic, isotherm adsorption and thermodynamic studies. *Biointerface Research in Applied Chemistry*, *11*(5), 12717-12731. https://doi.org/10.33263/BRIAC115.1271712731.

Kumari, K., Moldrup, P., Paradelo, M., Elsgaard, L., & de Jonge, L. W. (2016). Soil properties control glyphosate sorption in soils amended with birch wood biochar. *Water, Air, & Soil Pollution*, *227*(6), 1-12. https://doi.org/10.1007/s11270-016-2867-2.

Lita, A., Maulana, A., & Ryswaldi, R. (2022). Characteristics Biochar from Young Coconut Waste based on Particle Size as Améliorant. IOP Conference Series: Earth and Environmental Science, https://doi.org/10.1088/1755-1315/959/1/012034

López-Luna, J., Ramírez-Montes, L. E., Martinez-Vargas, S., Martínez, A. I., Mijangos-Ricardez, O. F., González-Chávez, M. d. C. A., . . . Vázquez-Hipólito, V. (2019). Linear and nonlinear kinetic and isotherm adsorption models for arsenic removal by manganese ferrite nanoparticles. *SN Applied Sciences*, *1*(8), 950. https://doi.org/10.1007/s42452-019-0977-3.

Ma'ruf, A., Pramudono, B., & Aryanti, N. (2017). Lignin isolation process from rice husk by alkaline hydrogen peroxide: Lignin and silica extracted. AIP Conference Proceedings, https://doi.org/10.1063/1.4978086

Maggi, F., la Cecilia, D., Tang, F. H., & McBratney, A. (2020). The global environmental hazard of glyphosate use. *Science of the total environment*, *717*, 137167. https://doi.org/10.1016/j.scitotenv.2020.137167.

Maulana, A., Herviyanti, Prasetyo, T., Harianti, M., & Lita, A. (2022). Effect of Pyrolysis Methods on Characteristics of Biochar from Young Coconut Waste as Ameliorant. IOP Conference Series: Earth and Environmental Science, https://doi.org/10.1088/1755-1315/959/1/012035

Maulana, A., Prima, S., Rezki, D., Sukma, V., Fitriani, A., & Herviyanti. (2021). Carbon sequestration from bamboo biochar on the productivity of ultisols and soybean [Glycine max L.] plants. IOP Conference Series: Earth and Environmental Science, https://doi.org/10.1088/1755-1315/741/1/012025

Mindari, W., Aini, N., Kusuma, Z., & Syekhfani, S. (2014). Effects of humic acid-based cation buffer on chemical characteristics of saline soil and growth of maize. *Journal of Degraded and Mining Lands Management*, *2*(1), 259. https://doi.org/10.15243/jdmlm.2014.021.259.

Mujinya, B., Van Ranst, E., Verdoodt, A., Baert, G., & Ngongo, L. (2010). Termite bioturbation effects on electro-chemical properties of Ferralsols in the Upper Katanga (DR Congo). *Geoderma*, *158*(3-4), 233-241. https://doi.org/10.1016/j.geoderma.2010.04.033.

Okada, E., Costa, J. L., & Bedmar, F. (2016). Adsorption and mobility of glyphosate in different soils under no-till and conventional tillage. *Geoderma*, *263*, 78-85. https://doi.org/10.1016/j.geoderma.2015.09.009.

Orcelli, T., di Mauro, E., Urbano, A., Valezi, D. F., da Costa, A., Zaia, C. T. B., & Zaia, D. A. (2018). Study of interaction between glyphosate and goethite using several methodologies: an environmental perspective. *Water, Air, & Soil Pollution*, *229*(5), 1-18. https://doi.org/10.1007/s11270-018-3806-1.

Pereira, R. C., Anizelli, P. R., Di Mauro, E., Valezi, D. F., da Costa, A. C. S., Zaia, C. T. B., & Zaia, D. A. (2019). The effect of pH and ionic strength on the adsorption of glyphosate onto ferrihydrite. *Geochemical transactions*, *20*(1), 1-14. https://doi.org//10.1186/s12932-019-0063-1.

Pereira, R. C., da Costa, A. C., Ivashita, F. F., Paesano Jr, A., & Zaia, D. A. (2020). Interaction between glyphosate and montmorillonite in the presence of artificial seawater. *Heliyon*, *6*(3), e03532. https://doi.org/10.1016/j.heliyon.2020.e03532.

Premarathna, K., Rajapaksha, A. U., Adassoriya, N., Sarkar, B., Sirimuthu, N. M., Cooray, A., . . . Vithanage, M. (2019). Clay-biochar composites for sorptive removal of tetracycline antibiotic in aqueous media. *Journal of* *environmental management*, *238*, 315-322. https://doi.org/10.1016/j.jenvman.2019.02.069.

Preocanin, T., Abdelmonem, A., Montavon, G., & Luetzenkirchen, J. (2016). Charging behavior of clays and clay minerals in aqueous electrolyte solutions—experimental methods for measuring the charge and interpreting the results. In G. M. do Nascimento (Ed.), *Clays, Clay Minerals and Ceramic Materials Based on Clay Minerals* (pp. 51-88). IntechOpen. https://doi.org/10.5772/62082

Shaaban, A., Se, S.-M., Mitan, N. M. M., & Dimin, M. (2013). Characterization of biochar derived from rubber wood sawdust through slow pyrolysis on surface porosities and functional groups. *Procedia Engineering*, *68*, 365-371. https://doi.org/10.1016/j.proeng.2013.12.193.

Sidoli, P., Baran, N., & Angulo-Jaramillo, R. (2016). Glyphosate and AMPA adsorption in soils: laboratory experiments and pedotransfer rules. *Environmental Science and Pollution Research*, *23*(6), 5733-5742. https://doi.org/10.1007/s11356-015-5796-5.

Singh, B., Camps-Arbestain, M., & Lehmann, J. (2017). *Biochar: a guide to analytical methods*. CRC Press, Boca Raton, FL, USA. https://doi.org/10.1111/sum.12389

Sudirja, R., Arifin, M., & Joy, B. (2015). Adsorpsi Paraquat dan Sifat Tanah pada Tiga Subgrup Tanah Akibat Pemberian Amelioran. *Agrikultura*, *26*(1), 41-48. https://doi.org/10.24198/agrikultura.v26i1.8459.

Tévez, H. R., & Afonso, M. d. S. (2015). pH dependence of Glyphosate adsorption on soil horizons. *Boletín de la Sociedad Geológica Mexicana*, *67*(3), 509-516. https://www.scielo.org.mx/scielo.php?script=sci_arttext&pid=S1405-33222015000300013.

Trigo, C., Cox, L., & Spokas, K. (2016). Influence of pyrolysis temperature and hardwood species on resulting biochar properties and their effect on azimsulfuron sorption as compared to other sorbents. *Science of the total environment*, *566*, 1454-1464. https://doi.org/10.1016/j.scitotenv.2016.06.027.

Tsamo, C., Assabe, M., Argue, J., & Ihimbru, S. (2019). Discoloration of methylene blue and slaughter house wastewater using maize cob biochar produced using a constructed burning chamber: a comparative study. *Scientific African*, *3*, e00078. https://doi.org/10.1016/j.sciaf.2019.e00078.

Tzanetou, E., & Karasali, H. (2020). Glyphosate Residues in Soil and Air: An Integrated Review. In D. Kontogiannatos, A. Kourti, & K. F. Mendes (Eds.), *Pests, Weeds and Diseases in Agricultural Crop and Animal Husbandry Production*. IntechOpen. https://doi.org/10.5772/intechopen.93066

Varjani, S., Kumar, G., & Rene, E. R. (2019). Developments in biochar application for pesticide remediation: current knowledge and future research directions. *Journal of environmental management*, *232*, 505-513. https://doi.org/10.1016/j.jenvman.2018.11.043.

Viglašová, E., Galamboš, M., Danková, Z., Krivosudský, L., Lengauer, C. L., Hood-Nowotny, R., . . . Briančin, J. (2018). Production, characterization and adsorption studies of bamboo-based biochar/montmorillonite composite for nitrate removal. *Waste Management*, *79*, 385-394. https://doi.org/10.1016/j.wasman.2018.08.005.

Wang, X., Gu, Y., Tan, X., Liu, Y., Zhou, Y., Hu, X., . . . Liu, S. (2019). Functionalized biochar/clay composites for reducing the bioavailable fraction of arsenic and cadmium in river sediment. *Environmental toxicology and chemistry*, *38*(10), 2337-2347. https://doi.org/10.1002/etc.4542.

Yao, Y., Gao, B., Fang, J., Zhang, M., Chen, H., Zhou, Y., . . . Yang, L. (2014). Characterization and environmental applications of clay–biochar composites. *Chemical Engineering Journal*, *242*, 136-143. https://doi.org/10.1016/j.cej.2013.12.062.

Zhan, H., Feng, Y., Fan, X., & Chen, S. (2018). Recent advances in glyphosate biodegradation. *Applied microbiology and biotechnology*, *102*(12), 5033-5043. https://doi.org/10.1007/s00253-018-9035-0.